Crystal Structure of the Kringle 2 Domain of Tissue Plasminogen Activator at 2.4-Å Resolution†

Abraham M. de Vos,*,‡ Mark H. Ultsch,‡ Robert F. Kelley,‡ Kaillathe Padmanabhan,§ Alexander Tulinsky,§ Mary L. Westbrook,∥ and Anthony A. Kossiakoff‡

Department of Protein Engineering, Genentech, Inc., 460 Point San Bruno Boulevard, South San Francisco, California 94080, Department of Chemistry, Michigan State University, East Lansing, Michigan 48824, and Biological and Medical Research, Argonne National Laboratory, Argonne, Illinois 60439

Received June 19, 1991; Revised Manuscript Received September 3, 1991

ABSTRACT: The crystal structure of the kringle 2 domain of tissue plasminogen activator was determined and refined at a resolution of 2.43 Å. The overall fold of the molecule is similar to that of prothrombin kringle 1 and plasminogen kringle 4; however, there are differences in the lysine binding pocket, and two looping regions, which include insertions in kringle 2, take on very different conformations. Based on a comparison of the overall structural homology between kringle 2 and kringle 4, a new sequence alignment for kringle domains is proposed that results in a division of kringle domains into two groups, consistent with their proposed evolutionary relation. The crystal structure shows a strong interaction between a lysine residue of one molecule and the lysine/fibrin binding pocket of a noncrystallographically related neighbor. This interaction represents a good model of a bound protein ligand and is the first such ligand that has been observed in a kringle binding pocket. The structure shows an intricate network of interactions both among the binding pocket residues and between binding pocket residues and the lysine ligand. A lysine side chain is identified as the positively charged group positioned to interact with the carboxylate of lysine and lysine analogue ligands. In addition, a chloride ion is located in the kringle–kringle interface and contributes to the observed interaction between kringle molecules.

Kringles are independent structural and functional folding domains found in regulatory proteases involved in blood coagulation and fibrinolysis (Sottrup-Jensen et al., 1978; Patthy, 1985). Kringle sequences have been recognized in prothrombin (PT)[1] (2 copies; Magnussen et al., 1975), plasminogen (PL) (5 copies; Magnussen et al., 1976), apolipoprotein(a) (38 copies; McLean et al., 1987), hepatocyte growth factor (4 copies; Nakamura et al., 1989), and tissue-type (Pennica et al., 1983) and urokinase-type (Steffens et al., 1982) plasminogen activators (t-PA and u-PA, with 2 and 1 copies, respectively). Kringles are essential for the biological activity and control of PT, PL, and t-PA; their exact function in the other proteins is as yet unclear. They are thought to interact with specific target proteins and/or small molecule ligands, thereby providing specificity to and regulation of their parent proteins. For example, the second kringle domain of t-PA (Van Zonneveld et al., 1986a; Ichinose et al., 1986; Higgins et al., 1987; Cleary et al., 1989) and the first and fourth kringles of PL (Thorsen, 1975; Thorsen et al., 1981) have high binding affinity for lysine and lysine analogues, and for fibrin. In the case of fibrin binding, it is assumed that an exposed lysine side chain of fibrin is the specific ligand.

t-PA is a serine protease involved in fibrinolysis [for a review see Kluft (1988)]. Its function is to convert PL into plasmin, which in turn degrades the fibrin in blood clots. The large enhancement of the activation of PL in the presence of fibrin or fibrin fragments (Hoylaerts et al., 1982) is thought to result from the high affinity of both t-PA and PL for fibrin. In t-PA, domain deletion studies have implicated the finger, growth factor, and second kringle domains in fibrin binding (Van Zonneveld et al., 1986a,b; Verheijen et al., 1986); a recent study using site-directed mutagenesis has demonstrated that, in addition, the first kringle domain and the protease domain are involved in interactions with fibrin and that the importance of kringle 2 for fibrin binding may be less than previously thought (Bennett et al., 1991). These findings all indicate that fibrin binding is a complicated process, involving more than one domain of t-PA.

Three-dimensional structures have been determined for the kringle 1 domain of PT fragment 1 (Tulinsky et al., 1988a), and for PL kringle 4, both without bound ligand (Mulichak & Tulinsky, 1991; Mulichak et al., 1991) and complexed with ε-amino caproic acid (ACA) (Wu et al., 1991). These structures delineate the basic characteristics of the binding pocket of kringles, while confirming the identification by chemical modification studies of some of the residues involved in lysine binding (Trexler et al., 1982; Vâli & Patthy, 1984). The lysine binding site in kringle 4 consists of a groove at the surface of the molecule, formed by two tryptophan side chains, flanked by charged residues: two aspartates interacting with the Nζ of the bound ACA ligand and two positively charged residues positioned to interact with the negatively charged carboxylate of lysine analogues. For the t-PA kringle-2, modeling attempts based on the structure of PT kringle 1 (Tulinsky et al., 1988b) were complicated by the fact that kringle 2 has three insertions compared to kringle 1 and kringle 4. Binding pocket residues in kringle 2 were thought to include tryptophans 62[2] and 72 and aspartates 55 and 57, but residues

† Some of this work was supported by NIH Grant HL25942 to A.T.
* To whom correspondence should be addressed.
‡ Genentech, Inc.
§ Michigan State University.
∥ Argonne National Laboratory.

[1] Abbreviations: t-PA, tissue plasminogen activator, u-PA, urokinase-type plasminogen activator; PT, prothrombin; PL, plasminogen.

[2] The numbering scheme adopted in this paper is based on the sequence of plasminogen kringle 5. The first cysteine of the kringle fold proper is numbered 1, and the last cysteine, 80. Insertions are numbered by appending an alphabetic character to the number of preceding residue, for example, Lys(47a). Residues preceding Cys(1) are denoted by residue numbers less than 1: Ser(−1), Asp(0).

0006-2960/92/0431-270$03.00/0

corresponding to the PL binding pocket arginines were not conclusively identified.

Here, we present the crystal structure of the kringle 2 domain of t-PA, determined using the method of multiple isomorphous replacement, and refined at 2.43-Å resolution. The overall three-dimensional structure is compared to that of PL kringle 4, and a new sequence alignment for kringle domains is proposed. The lysine binding pocket is described in detail and the structure is correlated to the results of recent mutational studies (Weening-Verhoeff et al., 1990; Bennett et al., 1991; Kelley et al., 1991).

Experimental Procedures

Structure Determination. Protein was expressed and purified as described by Cleary et al. (1989). Crystals were grown by vapor diffusion from a solution containing 4 mg/mL protein, 7% saturated NH_4Cl, and 50 mM NH_4HCO_3, pH = 8.0, and were determined to be monoclinic, space group $P2_1$ with a = 54.80 Å, b = 63.58 Å, c = 46.58 Å, and β = 106.73°, with three molecules per asymmetric unit. All intensity data sets used in the structure determination and preliminary refinement were collected on a Rigaku AFC6 diffractometer with CuKα radiation at 50 kV, 180 mA, using a peak-top step scan algorithm (Wyckoff et al., 1967) to obtain integrated intensities. Intensities were corrected for decay in a θ- and time-dependent manner, and for absorption by an empirical method (North et al., 1968). Three crystals were used to produce a 2.8-Å resolution native data set [$R_{merge}(I)$=0.087], consisting of 7103 unique reflections with $I > 0$ (92% completeness).

The structure was solved using the technique of multiple isomorphous replacement after initial attempts at molecular replacement using PL kringle 4 were unsuccessful. Three heavy atom derivatives were prepared by soaking crystals for a period of about 4 days in 6 mM $(NH_4)_2PtCl_4$ or 10 mM K_2AuCl_4 or a 200-fold dilution of a saturated KI solution, and a 3-Å data set was collected for each of these. Heavy atom positions were determined from difference Patterson maps, and origin and handedness correlation were established with difference Fourier maps. Phase refinement (with the PROTEIN package; Steigemann, 1982) was started with a total of 7 heavy atom sites; alternate cycles of refinement and difference Fourier calculations resulted in the inclusion of 11 minor sites (Table I) and produced a final figure of merit of 0.44 (6111 reflections in the resolution range 26–3.0 Å). Phases were improved by density modification using solvent flattening (Wang, 1985). The resulting electron density map clearly showed the molecular boundaries for three molecules in the asymmetric unit and good connectivity for most of the main chain. Map averaging was not applied, since interpretation of the map using the structure of PL kringle 4 as a model was straightforward, although it was immediately evident that there were substantial changes in some of the loop regions. The starting model for the subsequent refinement was obtained by replacing the sequence of kringle 4 by that of kringle 2, and by readjustment and refitting to the electron density map. Density for the termini was unclear, so that the six N-terminal residues and the two C-terminal residues were excluded from the starting model.

Crystallographic Refinement. All refinement was carried out with the program package X-PLOR (Brünger, 1990), using a low-resolution cutoff of 10 Å. Initial refinement was done with the 2.8-Å diffractometer data set, excluding the weakest 367 reflections from the refinement. The R factor for the starting model was 0.47 (10–3.5 Å); three iterations of refinement and map fitting, followed by the inclusion of 18 of the missing residues, decreased the R factor to 0.199 (10–2.8 Å). Refinement of tightly restrained individual temperature factors (R = 0.184) was followed by identification in a difference map (Figure 1a) of three chloride ions[3] (one in each molecule) that bound at the same positions as the three major sites of the KI derivative. Twenty water molecules were also identified. A subsequent round of refinement led to an R factor of 0.169.

Table I: Crystallographic Statistics

	resolution (Å)	no. of unique reflections	R_C[a]	phasing power[b]	no. of sites
Structure Determination					
native	2.8	7103			
$(NH_4)PtCl_4$	3.0	5934	0.612	1.38	10
K_2AuCl_4	3.2	4436	0.580	1.42	10
KI	3.0	5953	0.643	1.58	7

Refinement Data Set						
resolution (Å)	4.29	3.40	2.97	2.70	2.51	2.36
completeness (%)	94	95	97	97	86	60
average I/σ_I	77	49	23	12	7.0	4.4

Refinement	
resolution (Å)	10.0–2.43
no. of reflections	9687
crystallographic R	0.184
no. of protein atoms	2025
no. of water molecules	92
no. of chloride ions	3
rms deviation in bond lengths (Å)	0.016
rms deviation in bond angles (deg)	3.30
rms deviation in torsion angles (deg)	26
NCS[c] restraints on temperature factors (Å^2)	
main-chain atoms	2.0
side-chain atoms	2.5

[a] Cullis R-factor for centric reflections. [b] Phasing power: mean value of heavy atom structure factor amplitude divided by residual lack-of-closure error. [c] NCS: noncrystallographic symmetry.

The resulting model was used as the starting point for refinement with a new, 2.36-Å data set collected with a Siemens Area Detector at the Midwest Area Detector Facility at Argonne National Laboratory (Table I). The data set was processed with the XENGEN package of programs (Howard et al., 1987) and consisted of 11 623 unique reflections (30 526 observations averaged with R_{sym} = 0.068). In the shell at 2.43-Å resolution, the completeness of reflections with $F > 4\sigma_F$ was about 35%; this was chosen as the high-resolution cutoff for refinement, giving 9675 reflections with $F > 4\sigma_F$ between 10 and 2.43 Å. In the initial stages of refinement (10–2.8 Å), tight noncrystallographic symmetry (NCS) restraints were applied to the main-chain and side-chain atoms of residues Cys(1)–Ser(81) in each molecule; in addition, the individual temperature factors of equivalent atoms were tightly restrained to be similar. Inspection of the results (R = 0.184) led to the identification of four residues [Met(28), Gln(38), Arg(69), and Arg(70)] whose side chains appeared to adopt a different conformation in each molecule; thus, these side chains were no longer restrained to be similar. The next stage of refinement (10–2.43 Å) employed tight NCS restraints for the main-chain atoms of residues 1–81 and loose restraints for

[3] The identification of three strong peaks in the difference Fourier was made on the basis of the following considerations: (i) chloride and iodide bind strongly to kringle 2 and precipitate kringle 2 from solution, (ii) chloride was necessary for crystals to form, (iii) the peaks were in the interface between kringle molecules, (iv) the peaks were at the same positions as the three major heavy atom sites of the potassium iodide soak, and (v) the coordination around the chloride is consistent with examples found in crystal structures of amino acids.

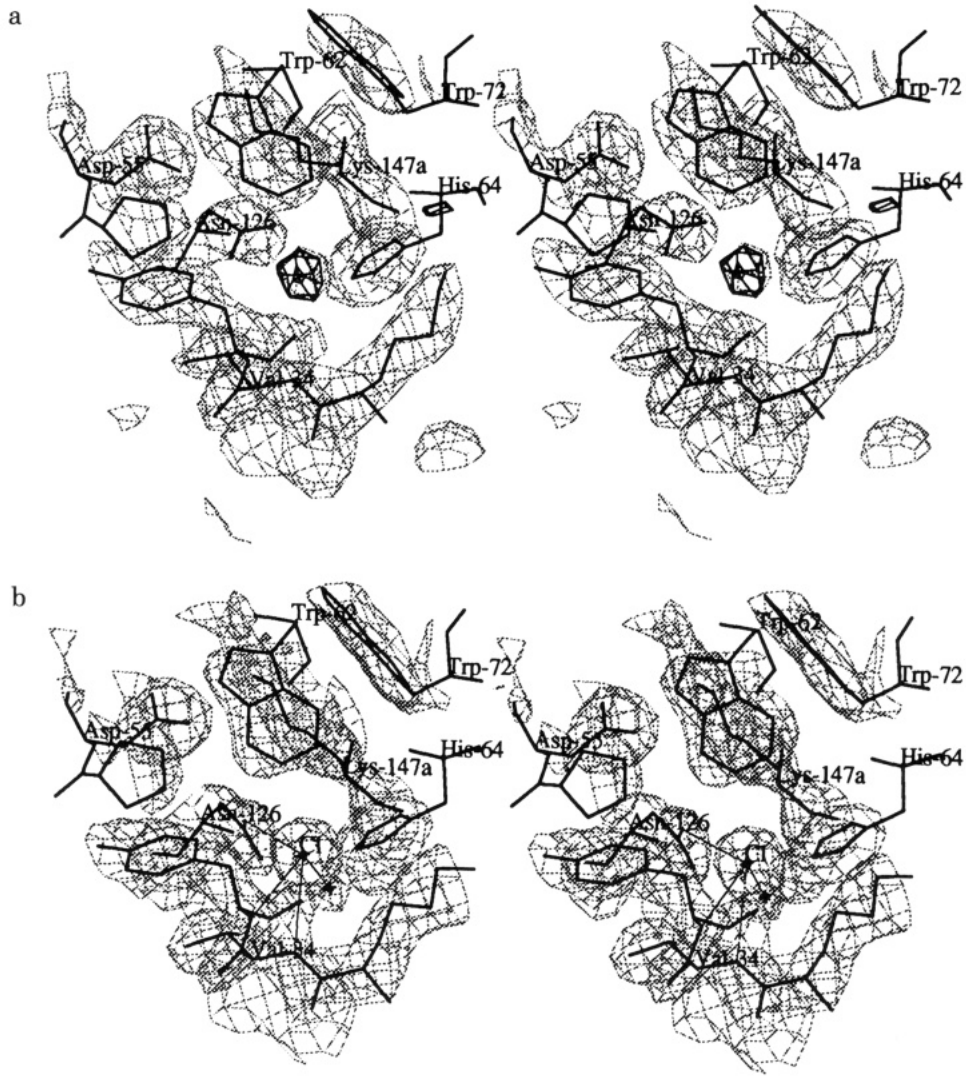

FIGURE 1: Environment of the chloride ion. Selected residues are labeled with residues from an adjacent molecule denoted as Lys-147(a) and Asn-126. (a) The 2.8-Å model used to identify the chloride ions is superimposed on its $2F_o - F_c$ map (gray lines). $F_o - F_c$ density assigned to the chloride is shown in thick lines. (b) The final model, including the chloride and an unlabeled water molecule, is superimposed on an omit $2F_o - F_c$ map (2.43-Å resolution). Hydrogen bonds involving the chloride are shown as thin lines.

the side-chain atoms, resulting in an R factor of 0.205. From this point, the side chain of residue Gln(42a) was also excluded from the NCS restraints, and additional cycles of refinement and difference Fourier calculations led to the identification of 72 more water molecules and an R factor of 0.184 (R = 0.209 for 10 563 reflections with $F > 0$). The final model consists of 2025 protein atoms out of a total of 2067, 3 chloride ions, and 92 water molecules, and the corresponding refinement statistics are summarized in Table I. The model has good stereochemistry for the protein molecules, with rms deviations in bond lengths and angles of 0.016 Å and 3.3°, respectively. The rms deviations among equivalent NCS-restrained main-chain atoms and side-chain atoms of the three independent molecules are 0.3 and 0.5 Å, respectively.

Results and Discussion

Crystal Packing Interactions. The three molecules that are found in the asymmetric unit of the kringle 2 crystals are related by a noncrystallographic 3-fold screw axis (Figure 2) that is nearly parallel to the crystal a-axis, with a transformation from molecule B to molecule A of 126° and 36 Å, and from molecule C to A of 122° and 18 Å. Of considerable biological interest is that the three noncrystallographically related molecules interact with each other mainly through their lysine/fibrin pockets: Lys(47a) of one molecule binds into the pocket of a neighboring molecule, in a manner fully consistent with the current understanding of these interactions, and similar to the ligand in the PL kringle 4–ACA complex (Wu et al., 1991). Thus, the present structure can serve as a model of the functional protein–protein interaction taking place between kringles and fibrin. That this interaction is the most important packing interaction in the crystal is consistent with the observation that the crystals grow most readily in the direction of this interaction (parallel to the crystallographic a-axis). It is noteworthy that the ready precipitation of t-PA might be the result of this same interaction between kringle 2 domains, since it can be kept in solution by the addition of lysine or arginine.

Description of the Structure. Like the PT kringle 1 and the PL kringle 4, the t-PA kringle 2 consists of four main loop structures. The loops are held together by three disulfide bonds in a characteristic pattern, two disulfide bonds in van der Waals contact with each other buried in the core of the molecule and one connecting the N- and C-termini. Comparison among the three molecules of the kringle fold proper [residues Cys(1)–Cys(80)] reveals that the molecules have very similar main-chain conformations, with an rms difference among main-chain atoms of 0.3 Å. The two N-terminal residues [Ser(−6), Glu(−5)] are disordered and were not in-

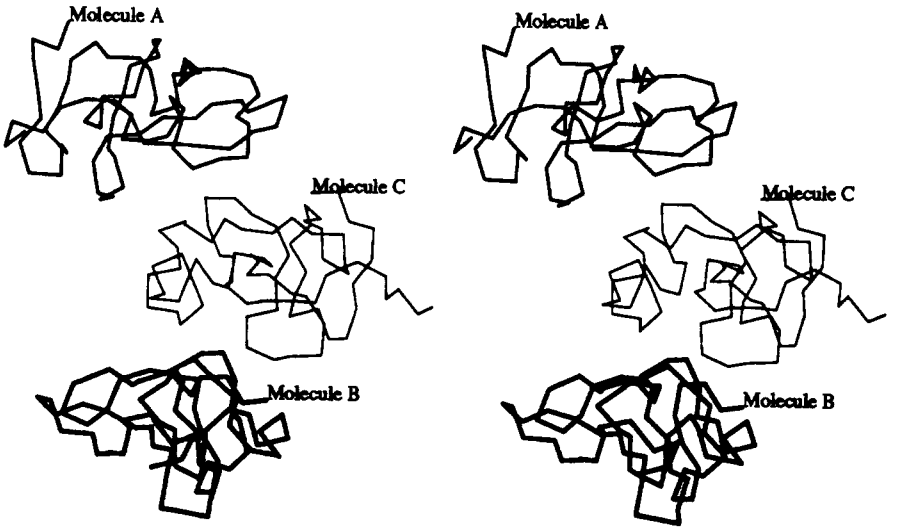

FIGURE 2: Stereoview of the crystal packing for Cα structures of the three noncrystallographically related molecules in the asymmetric unit of crystals of kringle 2. Molecules are related by a pseudo 3_1 screw axis, parallel to the crystallographic *a*-axis. Molecules are denoted A–C and labeled at their N-termini.

cluded in the model. The residues preceding and following the kringle fold proper, Gly(−3)–Asp(0) and Ser(81)–Thr(82), take on very different conformations in the three molecules and appear to be partially disordered, as evidenced by weak electron density and relatively high temperature factors ($B >$ 40 Å^2). The secondary structure found in kringle 2 in the crystal is similar to that determined from two-dimensional ^{1}H NMR measurements (Byeon et al., 1991). The only extensive β-sheet interaction found in the crystal structure is a two-stranded antiparallel β-ribbon formed by residues Pro(61)–Lys(67) and Arg(70)–Cys(75). Very short stretches of β-sheet-like interactions, consisting of two main-chain hydrogen bonds only, are found between Arg(52) and Trp(62), and between Ser(14)–Thr(16) and Ala(20)–Cys(22). The structure contains one turn of rather irregular helix, formed by residues Ser(41)–Gly(45), with main-chain hydrogen bonds formed between 41 and 43, 41 and 44, 42 and 44, and 42 and 45.

Seven β-turns can be recognized: Phe(3)–Gly(6), Gly(6)–Tyr(9), Ile(16)–Ala(20), Pro(24)–Ser(27), Ser(27)–Leu(30), Leu(30)–Lys(33), and Lys(67)–Arg(70). Following the classification of Wilmot and Thornton (1988), 6–9, 16–20, 24–27, and 27–30 are type I β-turns, and 67–70 is type I′. Turn 3–6 has type II′ conformation, and 30–33 is a somewhat distorted type II turn. Most of these are consistent with the NMR results (Byeon et al., 1991), the only major differences being the assignment there of 6–9 as helical and 67–70 as a type II turn.

Almost all the side chains among the three independent molecules A–C have a similar conformation, with an rms difference among equivalent atoms of 0.5 Å. The exceptions are the side chains of Met(28), Gln(38), Gln(42a), Arg(69), and Arg(70), which have rather different conformations in all three molecules, and His(13), which is different in molecule B from A and C. Inspection of the environment of these residues reveals that the side chains of 28, 38, and 42a protrude into the solvent and are less well-ordered (having temperature factors >40 Å^2), whereas the side chains of 69 and 70 of molecules A and B, but not C, are involved in nonequivalent packing interactions. In molecule B, His(13) has $\chi_1 = -145°$ and $\chi_2 = -91°$ compared to $\chi_1 = -79°$ and $\chi_2 = -94°$ in A and C. In molecule B the side chain is not directly involved in any interactions with the remainder of the molecule, but in A and C it is positioned such that its Nδ1 can make a good hydrogen bond (2.8 Å) with the hydroxyl of Tyr(9). However, in these cases there is also a difference peak located at the position the imidazole occupies in B, indicating that in A and C the ring takes on two orientations separated by a rotation of 66° about the Cα–Cβ bond. In this second orientation, the side chain is accessible to solvent, consistent with assessments based on titration of its imidazole (Byeon et al., 1989).

The core of the kringle 2 structure is formed by a hydrophobic cluster of three tryptophan residues surrounded by aromatic and hydrophobic side chains. The side chain of Trp(25) is in van der Waals contact with and perpendicularly oriented to Trp(62), and a similar situation is found for the rings of Trp(62) and Trp(72). The side chain of His(64) is in contact with the edge of the ring of Trp(62) and the methyl groups of Leu(30) and the methylene groups of Lys(33). There is also an interaction between the ring of Trp(25) and one of the methyl groups of Leu(46). Other residues forming part of this hydrophobic cluster include Tyr(35), Tyr(74), and Leu(71). Short distances among many of these side chains were detected in NMR studies (Byeon et al., 1991).

Comparison with PL Kringle 4 and PT Kringle 1. Apart from the termini [Gly(−3)–Asp(0) and Ser(81)–Thr(82)], the overall fold of the kringle structures that have been determined thus far is very similar. The core of the kringle 2 superimposes well on that of the PT kringle 1 (Tulinsky et al., 1988a) and the PL kringle 4 (Mulichak & Tulinsky, 1991), with rms deviations in main-chain atoms of about 0.7 Å (Figure 3). A central hydrophobic region similar to that found in kringle 2 has also been described for PT kringle 1 and PL kringles 4 and 5 (Atkinson & Williams, 1990; Hochswender et al., 1983; Ramesh et al., 1987; Motta et al., 1987; Thewes et al., 1988). The long antiparallel β-ribbon found in kringle 2 [Pro(61)–Lys(67) and Arg(70)–Cys(75)] exists in a shortened form in both kringle 1 and kringle 4, but the one-turn helix in kringle 2 [Ser(41)–Gly(45)] is not present in either of these other kringles. It should be noted, however, that this helix is part of a looping region containing two one-residue insertions in kringle 2. Two regions having a very different conformation between kringle 2 and kringle 4 or kringle 1 are kringle 2 Met(28)–Glu(42a) and Leu(66)–Leu(70a) (Figure 3). Each of these looping regions contains more residues in the case of kringle 2 (Figure 4), the former two, the latter one. The large differences in these loops, together with complications arising from the fact that there are three molecules in the asymmetric

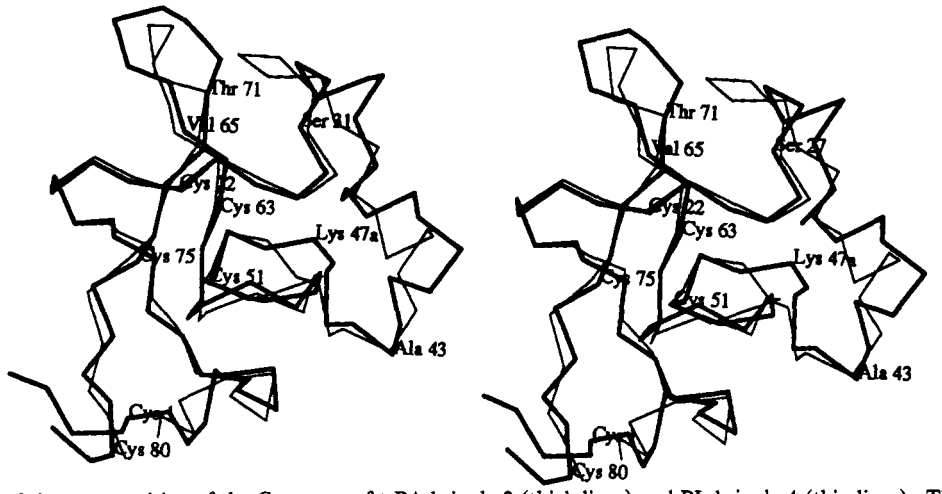

FIGURE 3: Stereoview of the superposition of the Cα atoms of t-PA kringle 2 (thick lines) and PL kringle 4 (thin lines). The positions of loops 27–43 and 65–71 are indicated, and the cysteines are labeled.

```
                    1        10        20        30        40        50
                    |        |         |         |         |         |
tPA K2       gnsdCYFGNGSAYRGTHSLTESGASCLPWNSmiligkvytaqnpsaqALGLgkHNYC
tPA K1     dtratCYEDQGISYRGTWSTAESGAECTNWNSsalaqkpysgrrpdaiRLGLgnHNYC
UKN K1     dksktCYEGNGHFYRGKASTDTMGRPCLPWNSatvlqqtyhahrsdalQLGLgkHNYC

PLA K4    tpvvqdCYHGDGQSYRGTSSTTTTGKKCQSWSSmtphrhqkt-penyp-NAGLt-MNYC
PLA K1     vylseCKTGDGKNYRGTMSKTKNGITCQKWSStsphrprfs-pathp-SEGLe-ENYC
PLA K2    leceeeCMHCSGENYDGKISKTMSGLECQAWDSqsphahgyi-pskfp-NKNLk-KNYC
PLA K3    sgptyqCLKGTGENYRGNVAVTVSGHTCQHWSAqtphthnrt-penfp-CKNLd-ENYC
PLA K5    tpseedCMFGNGKGYRGKRATTVTGTPCQDWAAqephrhsiftpetnp-RAGLe-KNYC
HGF K1   nkdyirnCIIGKGRSYKGTVSITKSGIKCQPWSSmiphehsfl-pssyr-GKDLq-ENYC
HGF K2         veCMTCNGESYRGLMDHTESGKICQRWDHqtphrhkfl-peryp-DKGFd-DNYC
HGF K3 dvpletteCIQGQGEGYRGTVNTIWNGIPCQRWDSqyphehdmt-penfk-CKDLr-ENYC
HGF K4      hgqdCYRGNGKNYMGNLSQTRSGLTCSMWDKnmedlhrhi-fwepd-ASKLn-ENYC
PRO K1   aaclegnCAEGLGTNYRGHVNITRSGIECQLWRSryphkpein-stthp-GADLq-ENFC
PRO K2    sppleqCVPDRGQQYQGRLAVTTHGLPCLAWASaqakalskh-qdfns-AVQLv-ENFC
```

(a)

```
                          60        70          80
                          |         |           |
tPA K2     RNPDGDA-KPWCHVlknrrlTWEYC-DVPSCst
tPA K1     RNPDRDS-KPWCYVfkagkySSEFC-STPACseg
UKN K1     RNPDNRR-RPWCYVqvglkpLVQEC-MVHDCadg

PLA K4     RNPDADK-GPWCFTtdpsv-RWEYC-NLKKCsgt
PLA K1     RNPDNDPqGPWCYTtdpek-RYDYC-DILECeee
PLA K2     RNPDREL-RPWCFTtdpnk-RWELC-DIPRCttp
PLA K3     RNPDGKR-APWCHTtnsqv-RWEYC-KIPSCdss
PLA K5     RNPDGDVgGPWCYTtnprk-LYDYC-DVPQCaap
HGF K1     RNPRGEEgGPWCFTsnpev-RYEVC-DIPQCsev
HGF K2     RNPDGQP-RPWCYTldpht-RWEYC-AIKTCadntmndt
HGF K3     RNPDGSE-SPWCFTtdpni-RVGYCSQIPNCdms
HGF K4     RNPDDDAhGPWCYTgnpli-PWDYC-PISRCegdttptivnl
PRO K1     RNPDSSNtGPWCYTtdptv-RRQEC-SIPVCgqd
PRO K2     RNPDGDEeGVWCYVagkpg-DFGYC-DLNYCeea
```

(b)

FIGURE 4: Sequence alignment for kringle domains based in the structures of t-PA kringle 2 and PL kringle 4. The first three kringles are proposed to have a structure similar to that of kringle 2, and the others, similar to kringle 4. Residues in upper case are structurally homologous between kringle 2 and kringle 4; residues in lower case are not. (a) Exon 1; (b) exon 2. Numbering adapted from Tulinsky et al. (1988a).

unit, are probably the reason for the failure of molecular replacement using kringle-4 as a model to solve the kringle-2 structure. A third insertion in kringle 2 [Lys(47a)] is accommodated without large changes in the surrounding residues.

Lysine Binding Pocket. Modeling studies combined with NMR results (Tulinsky et al., 1988b) and mutagenesis (Weenink-Verhoeff et al., 1990; Kelley et al., 1991) identified residues in kringle 2 that are thought to be involved in lysine binding and were complemented by the structure of the PL kringle 4–ACA complex (Wu et al., 1991). The binding pocket residues can be divided in three groups. The negatively charged side chains of Asp(55) and Asp(57) were proposed to be involved in interactions with the positively charged Nζ of the bound ligand, and the hydrophobic surface of Trp(62) was thought to form van der Waals contacts with its methylene groups. A positively charged residue, identified as Arg(71) in the case of the PL kringle 4, was proposed to interact with

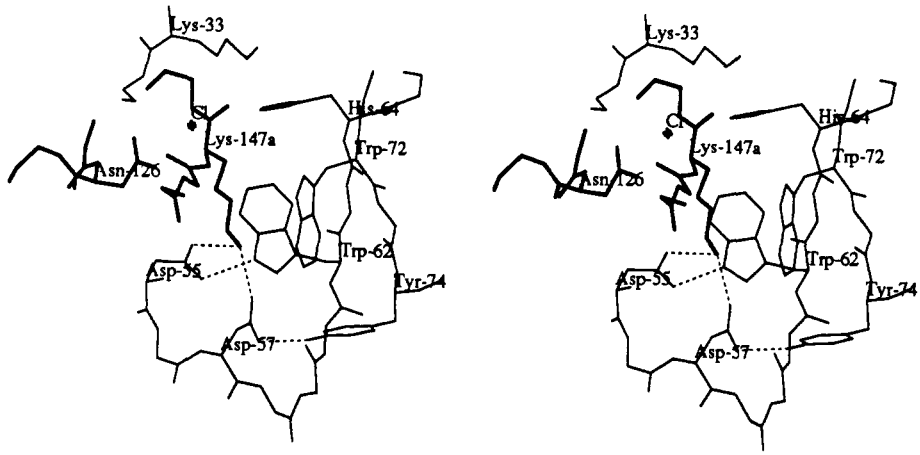

FIGURE 5: Stereoview of the lysine binding pocket of kringle 2. A neighboring molecule providing a lysine ligand is in thick lines; a chloride ion is designated with an asterisk. The bound ligand is labeled Lys(147a); binding pocket residues shown are Lys(33), Asp(55), Asp(57), His(64), Trp(62), Trp(72), and Tyr(74).

the negatively charged carboxylate of lysine or lysine analogues, although a corresponding residue in kringle 2 was not conclusively identified; His(64) was suggested (Tulinsky et al., 1988b), a residue which appears to be important for the specificity of kringle 2 for different lysine analogues (Kelley et al., 1991).

The intermolecular interactions found between the independent molecules in the asymmetric unit of the crystal confirm and extend the current understanding of kringle ligand binding. The Oδ1 atoms of Asp(55) and Asp(57) are at a distance of 2.7 Å from Nζ of Lys(47a) of an adjacent molecule (Figure 5). In addition, these side chains are oriented by hydrogen bonds between 55–Oδ2 and Trp(62)-Nε1 (3.0 Å) and between 57–Oδ2 and Tyr(74)–Oη (2.8 Å), respectively. The former interaction was predicted on the basis of NMR studies (Byeon et al., 1989) and the kringle 2 absorption spectrum (M. G. Mulkerrin, personal communication). The ligand methylene groups are in contact with the side chains of Trp(62) and Trp(72). As also observed in kringle 4, these two tryptophan side chains are oriented perpendicular to each other, forming a groove in which the hydrophobic part of the ligand fits closely. The positively charged side chain proposed to interact with the negatively charged end of lysine analogues is shown by this structure to be Lys(33), whose terminal Nζ group is 2.9 Å from the carbonyl oxygen of the Lys(47a) ligand that is provided by an adjacent molecule. Contacting the methylene groups of Lys(33) and the edge of the ring of Trp(62), but not in direct contact with the ligand, is $C_{\epsilon 1}$ of His(64). Previous modeling attempts dismissed Lys(33) as the positively charged residue positioned to interact with the ligand carboxylate because its side chain was pointing in an unfavorable direction. Considering the large changes in the main chain of loop 28–42a compared to PT kringle 1, the oversight is to be expected.

The organization of the binding pocket is in good agreement with the results of mutational analysis of residues on the isolated kringle 2 domain (Table II). Thus, mutation of the critical aspartate residues at position 55 or 57 results in markedly decreased lysine binding, whereas the binding affinity of the G56R variant is similar to wild type. Similarly, removal of the positive charge interacting with the carboxylate of the ligand abolishes lysine binding (K33A mutant), while a change from lysine to arginine retains lysine binding affinity. Mutation of residues outside the binding pocket has little effect on lysine binding (K47aN, K60A, R69G, R70K, T71V/R); the structure shows these side chains to be at the surface of the molecule.

Table II: Lysine–Sepharose Binding of Kringle 2 Mutants[a]

mutant	lysine–Sepharose binding	mutant	lysine–Sepharose binding
wild type	+	D57N	–
K33A	–	H64Y	+
K33R	+	R69G	+
K47aN	+	R70K	+
K60A	+	T71V	+
D55N	–	T71R	+
G56R	+	W72S	–

[a] Kringle 2 mutants were constructed by oligonucleotide-directed mutagenesis and expressed by secretion in *Escherichia coli* as described previously (Kelley & Cleary, 1989). Crude extracts prepared from 25 mL of overnight *E. coli* cultures were loaded on a 2-mL lysine–Sepharose column. Lysine–Sepharose binding was assayed by measuring kringle 2 concentration in the load, flow-through, and ligand-eluted fraction by ELISA using a polyclonal antibody raised against t-PA. A "–" in the table indicates that more than 90% of the loaded protein was found in the flow-through fraction. Conversely, a "+" indicates that more than 70% of the loaded kringle 2 was found in the ligand-eluted fraction.

Kringle 1 of t-PA does not have appreciable lysine binding affinity (R. F. Kelley, unpublished results; Bennett et al., 1991). The only binding pocket residue that is different between kringle 1 and kringle 2 is at position 72, which is serine in kringle 1 and tryptophan in kringle 2. The lack of lysine binding affinity of the kringle 2 W72S mutation (Table II) is therefore unlikely to be caused by misfolding of the resulting mutant and would indicate that the contribution of the ring of Trp(72) is essential for lysine binding. Finally, the H64Y mutant showed wild-type-like lysine binding affinity. As noted above, the side chain of His(64), while not directly in contact with the ligand, does interact with Lys(33) and Trp(62); in this context, it is noteworthy that histidine, tyrosine, or phenylalanine is conserved at this position. Changes in specificity for various lysine analogues of the H64Y mutant have demonstrated the importance of this residue for lysine analogue binding (Kelley et al., 1991). Although the absence of structures of wild-type and mutant kringle 2 with lysine analogues bound makes it difficult to explain these results in any detailed manner, the contacts between the side chains of His(64) and Lys(33), and between His(64) and Trp(62), do support the observations in a general sense.

The second major interaction between kringle molecules found in the crystal structure is mediated via a chloride ion (its environment is shown in Figure 1b). This finding is in agreement with the observation that even relatively low concentrations of chloride will precipitate the protein (Figure 6),

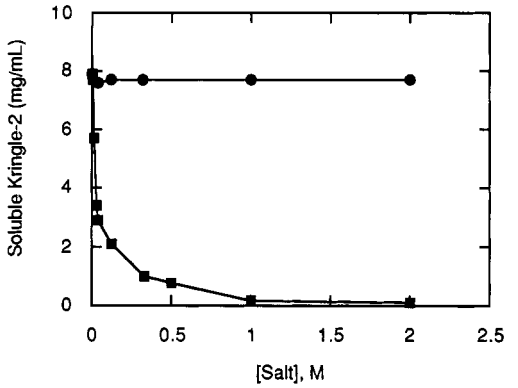

FIGURE 6: Precipitation of kringle 2 by chloride. Solutions containing 8 mg/mL kringle 2 and varying concentrations of either sodium acetate (filled circles) or sodium chloride (filled squares) were incubated overnight at ambient temperature with agitation on an orbital shaker. These solutions were centrifuged, and the concentration of kringle 2 remaining in the supernatant was determined by absorbance measurements.

and in fact, crystals could not be obtained without chloride. The ion is found at the edge of the binding pocket in the interface between two molecules. It is bound to the main-chain amides of residues Val(34) and Tyr(35), which are part of a loop surrounding the binding pocket (with Cl^--to-N distances of 3.2–3.3 Å), and to the side chain of Asn(26) of the adjacent liganding molecule. A water molecule serves as a fourth ligand (3.1 Å), which is in turn hydrogen-bonded to Oδ1 of Asn(26). These distances and coordination are in good agreement with those found in crystal structures of amino acids containing chloride ions (Jeffrey & Maluszynksa, 1982). In addition, the chloride ion is in van der Waals contact with the Cγ methylene group of Lys(33), as well as with $C_{\epsilon 1}$ of His(64), and its absence would leave a cavity in the interface that could presumably be filled with waters.

The physiological concentration of chloride (about 100 mM; Flear & Hughes, 1963) is well above the chloride concentration needed to precipitate the isolated kringle 2 domain from solution ($IC_{50} \approx 30$ mM: Figure 6). It is unknown whether fibrin and/or lysine analogue binding of t-PA is influenced by negative ions, but a chloride-induced conformational change has been proposed for plasminogen, inhibiting its activation by urokinase or t-PA (Urano et al., 1987, 1988). The observation that chloride is necessary for crystal formation of t-PA kringle 2 and the presence of the chloride ion at the edge of the lysine binding pocket in the interface between adjacent molecules suggest that this conformational change in plasminogen may be the result of an *intra*molecular interaction involving the lysine binding pocket of one of the kringle domains of that molecule. The observation that ACA can relieve the chloride-induced inhibition of plasminogen activation (Urano et al., 1987, 1988) is consistent with this hypothesis, since ACA would block the lysine binding pocket and prevent the interaction in question, just as in the case of kringle 2 addition of ACA solubilizes chloride-induced precipitate (R. F. Kelley, unpublished observations).

A comparison between kringle 2 and kringle 4 (Mulichak & Tulinsky, 1990) reveals that their lysine binding pockets are very similar (Figure 7). The position and orientation of most of the binding pocket residues are virtually identical, but the side chain of Trp(72) has moved by about 0.7 Å, and the orientation of Asp(57) is somewhat different. This may be the result of the fact that in the crystal structure of kringle 4 the binding pocket is partially occupied by an arginine side chain of a neighboring molecule, but not in a lysine-like binding mode (Mulichak & Tulinsky, 1990). Overall, this structural comparison together with tryptophan fluorescence and circular dichroism measurements (R. F. Kelley, unpublished results) indicating little or no conformational change in kringle 2 upon ACA binding supports the notion that the lysine binding pocket is preformed and does not require conformational changes upon ligand binding.

As noted above, the present structure resolves the uncertainty regarding the residue proposed to interact with the ligand carboxylate, found to be Arg(71) in kringle 4. In kringle 2 a residue from a different position in the sequence, Lys(33), is positioned to perform this function (Figure 5). Comparison of the structures shows that the position of the ϵ-amino group of kringle 2 Lys(33) is virtually identical to that of the guanidinium group of Arg(71) in kringle 4, providing an interesting example of structural, but not sequential homology.

His(64) in kringle 2 is important for ligand specificity (Kelley et al., 1991). Whereas in the kringle 2 structure the histidine side chain does not contact the ligand, in the case of the corresponding Phe(64) in the kringle 4–ACA complex the edge of the phenylalanine ring is in direct van der Waals contact with the Cα of the ligand. This structural difference

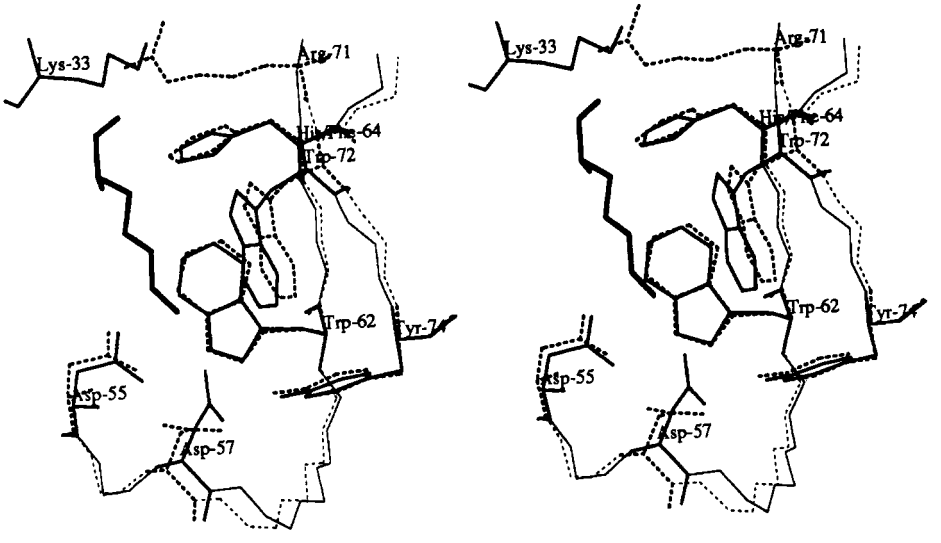

FIGURE 7: Stereoview of the superposition of the lysine binding pockets of t-PA kringle 2 (solid lines) and PL kringle 4 (dashed lines). Lys(47a) from an adjacent molecule is depicted in thick lines.

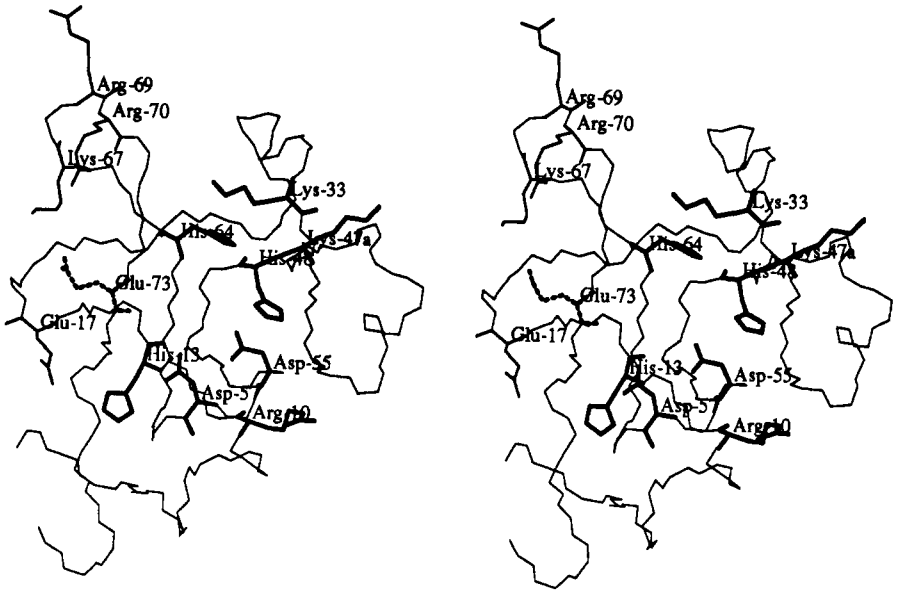

FIGURE 8: Stereoview of the backbone of kringle 2 showing only side chains that were modified in Bennett et al. (1991). Side chains concluded to be important for lysine or fibrin binding are in thick lines; side chains mutation of which did not decrease lysine and fibrin binding are in thin lines.

may have a bearing on the observed difference in chain-length specificity between kringle 2 and kringle 4 (Winn et al., 1980; Cleary et al., 1989), although structures of lysine analogue complexes bound to kringle 2 are needed for a more detailed investigation of this effect.

Correlation with Mutational Studies on t-PA. The effects of changes in kringle 2 on lysine and fibrin binding of t-PA were addressed in two recent site-directed mutagenesis studies (Weening-Verhoeff et al., 1990; Bennett et al., 1991). Lysine binding affinity of t-PA is mediated by its kringle 2 domain, but fibrin binding is a more complicated process (Bennett et al., 1991). Therefore, the effects of mutation on lysine binding are easier to interpret.

Of the residues changed (Figure 8), effects on lysine binding affinity were found only for residues in the binding pocket. Thus, changes in Asp(55) or Asp(57) that abolish the interaction with the positively charged end of the ligand result in loss of lysine binding affinity (Weening-Verhoeff et al., 1990; Bennett et al., 1991). The same effect is observed for the H64A variant (Bennett et al., 1991), consistent with the interactions observed between the imidazole ring and other binding pocket residues. However, in the light of the interaction observed in the crystal structue between Nζ of Lys(33) and the carbonyl oxygen of the ligand, it is unclear why lysine binding of the K33A variant was not affected similarly (Bennett et al., 1991); it should be noted the K33A variant of the isolated kringle 2 domain does not bind lysine (Table II).

Since binding to fibrin of t-PA is mediated only to a small extent by the kringle 2 domain (Bennett et al., 1991), the effect of changes in kringle 2 on fibrin binding affinity of t-PA is difficult to evaluate. Changes in fibrin binding of variants containing mutations in binding pocket residues (D55A, D57A, H64A; Bennett et al., 1991) are probably caused by abolishment of a direct kringle–fibrin interaction, although D55N and D57N variants have wild-type affinity (Weening-Verhoeff et al., 1990). As was observed for lysine binding, the K33A variant had wild-type fibrin binding affinity (Bennett et al., 1991). Mutations that resulted in decreased fibrin binding affinity, but unchanged lysine binding, were R10A and K47aA/H48A (Bennett et al., 1991). The same effect was observed when Glu(73) was changed to glutamine (Weening-Verhoeff et al., 1990), but not for the E73A variant (Bennett et al., 1991). Since all these residues are far removed from the lysine binding pocket, any effect of these changes on fibrin binding is likely to be indirect, possibly the disruption of *intra*molecular domain–domain interactions, resulting in a loss of binding affinity of another domain. The fact that Arg(10), Lys(47a), and Glu(73) are at the surface of the kringle 2 domain (Figure 8) is consistent with this rationalization. Finally, mutation of His(13), Glu(17), Lys(67), Arg(69), or Arg(70) did not affect fibrin binding affinity (Bennett et al., 1991); all these residues are far from the binding pocket and at the surface of the molecule (Figure 8).

Kringle Sequence Alignment. The structurally conserved segments of kringle 2 and kringle 4 can be used to propose a new alignment for kringle sequences (Figure 4). This alignment shows that kringle domains fall in two distinct groups. Kringles in the first group have the longer loop regions, 28–42a and 66–70a, that are seen in kringle 2, whereas the second group is characterized by the shorter segments found in kringle 4. Group 1, with the smaller number of kringles, consists of t-PA kringles 1 and 2 and the kringle domain from urokinase-type plasminogen activator. Group 2 contains the 5 PL kringles, the 2 PT kringles, the 4 hepatocyte growth factor kringle domains, and (not shown in Figure 4) the 38 kringles from apolipoprotein(a) (37 homologous to the PL kringle 4, and 1 to the PL kringle 5). The three-dimensional structure of kringles in group 1 probably resembles that of kringle 2, whereas kringles from group 2 are likely to be similar to PL kringle 4. This classification of kringle domains is consistent with their proposed evolutionary relation (Patthy et al., 1984; Patthy, 1985) and supported by the fact that each of the two exons identified in kringle domains contains one of the characteristic loops, indicating that exon swapping between groups has not taken place. It should be noted that fibrin/lysine binding functionality is not exclusive to either of the groups.

SUMMARY

The crystal structure of the t-PA kringle 2 shows an interaction between a lysine of one molecule and the lysine binding pocket of a neighbor. Many of the interactions between the ligand and the residues in this pocket predicted on

the basis of the structure of prothrombin kringle 1 are found in the kringle 2 structure, and a series of mutations in the isolated kringle 2 domain correlates well with the interactions observed between ligand and binding pocket residues. Therefore, the mode of binding observed in the kringle 2 crystal is likely to be a functional model of a protein ligand in a kringle binding pocket. The structure identifies the residue proposed to interact with the carboxyl end of kringle binding pocket ligands to be Lys(33), whose ϵ-amino group is found in a position equivalent to that of the guanidinium of Arg(71) in plasminogen kringle 4. A negatively charged chloride ion at the edge of the binding pocket contributes to kringle–kringle binding in the crystal, but its relevance for fibrin and lysine analogue binding is unclear. Correlation of the structure to the results of lysine and fibrin binding studies on t-PA variants containing clustered point mutations in the kringle 2 domain identifies residues possibly involved in *intra*molecular domain–domain interactions.

Comparison of the structures of kringle 2 and plasminogen kringle 4 shows that most of the fold is conserved, but that two segments of polypeptide chain have very different main-chain conformations. Alignment of all presently known kringle sequences on the basis of this structural comparison allows classification of kringle domains in two groups, the first containing all the plasminogen activator kringles, while the second contains all other kringle domains thus far identified. Whereas the plasminogen kringle 4 structure should provide a good model for kringles in this second group, the kringle 2 structure represents the basis for modeling not only of lysine analogue bound kringle 2 variants, but also of the other kringle domains of group 1.

ACKNOWLEDGMENTS

We thank Dr. Bruce Keyt for helpful discussions on kringle 2 mutations in t-PA.

Registry No. t-PA, 105913-11-9; Lys, 56-87-1; Cl^-, 16887-00-6.

REFERENCES

Atkinson, R. A., & Williams, R. J. P. (1990) *J. Mol. Biol. 212*, 541–552.

Bennett, W. F., Paoni, N. F., Keyt, B. A., Botstein, D., Jones, A. J. S., Presta, L., Wurm, F. M., & Zoller, M. J. (1991) *J. Biol. Chem. 266*, 5191–5201.

Byeon, I.-J. L., Kelley, R. F., & Llinás, M. (1989) *Biochemistry 28*, 9350–9360.

Byeon, I.-J. L., Kelley, R. F., & Llinás, M. (1991) *Eur. J. Biochem. 197*, 155–165.

Brünger, A. T. (1990) *X-PLOR manual, Version 1.5*, 2nd printing, Yale University, New Haven.

Cleary, S., Mulkerrin, M. G., & Kelley, R. F. (1989) *Biochemistry 28*, 1884–1891.

Flear, C. T. G., & Hughes, P. (1963) *Br. Heart J. 25*, 166–172.

Higgins, D. L., & Vehar, G. A., (1987) *Biochemistry 26*, 7786–7791.

Hochswender, S. M., Laursen, R. A., De Marco, A., & Llinás, M. (1983) *Arch. Biochem. Biophys. 223*, 58–67.

Howard, A. J., Gilliland, G. L., Finzel, B. C., Poulos, T. L., Ohlendorf, D. H., & Salemme, F. R. (1987) *J. Appl. Cryst. 20*, 383–387.

Hoylaerts, M., Rijken, D. C., Lijnen, H. R., & Collen, D. (1982) *J. Mol. Chem. 257*, 2912–2929.

Ichinose, A., Takio, K., & Fujikawa, K. (1986) *J. Clin. Invest. 78*, 163–169.

Jeffrey, G. A., & Maluszynska, H. (1982) *Int. J. Biol. Macromol. 4*, 173–185.

Kelley, R. F., de Vos, A. M., & Cleary, S. (1991) *Proteins: Struct., Funct., Genet. 11*, 35–44.

Kluft, C. (1988) in *Tissue-Type Plasminogen Activator (t-PA): Physiological and Clinical Aspects* (Kluft, C., Ed.) Vol. 1, pp 47–82, CRC Press, Boca Raton, FL.

Magnussen, S., Petersen, T. E., Sottrup-Jensen, L., & Claeys, H. (1975) in *Proteases and Biological Control* (Reich, E., Rifkin, D. B., & Shaw, E., eds.) pp 123–149, Cold Spring Harbor Laboratory Press, Cold Spring Harbor, NY.

Magnussen, S., Sottrup-Jensen, L., Petersen, T. E., Dudek-Wojciechowska, G., & Claeys, H. (1976) in *Proteolysis and Physiological Regulation* (Robbins, D. W., & Braw, K., eds.) pp 203–208, Academic Press, NY.

McLean, J. W., Tomlinson, J. E., Kuang, W.-J., Eaton, D. L., Chen, E. Y., Fless, G. M., Scanu, A. M., & Lawn, R. M. (1987) *Nature 330*, 132–137.

Motta, A., Laursen, R. A., Llinás, M., Tulinsky, A., & Park, C. H. (1987) *Biochemistry 26*, 3827–3836.

Mulichak, A. M., & Tulinsky, A. (1990) *Blood Coag. Fibrinol. 1*, 673–679.

Mulichak, A. M., Tulinsky, A., & Ravichandran, K. G. (1991) *Biochemistry* (in press).

Nakamura, T., Nishizawa, T., Hagiya, M., Seki, T., Shimonishi, M., Sugimura, A., Tashiro, K., & Shimizu, S. (1989) *Nature 342*, 440–443.

North, A. C. T., Phillips, D. C., & Mathews, F. S. (1968) *Acta Crystallogr. A24*, 351–359.

Patthy, L. (1985) *Cell 41*, 657–663.

Patthy, L., Trexler, M., Váli, Z., Bányia, L., & Váradi, A. (1984) *FEBS Lett. 171*, 131–136.

Pennica, D., Holmes, W. E., Kohr, W. J., Harkins, R. N., Vehar, G. A., Ward, C. A., Bennet, W. F., Yelverton, E., Seeburg, P. H., Heyneker, H. L., & Goeddel, D. V. (1983) *Nature 301*, 214–220.

Ramesh, V., Petros, A. M., Llinás, M., Tulinsky, A., & Park, C. H. (1987) *J. Mol. Biol. 198*, 481–498.

Sottrup-Jensen, L., Claeys, H., Zajdel, M., Petersen, T. E., & Magnussen, S. (1978) in *Progress in Chemical Fibrinolysis and Thrombolysis* (Davidson, J. F., et al., Eds.) Vol. 3, pp 191–209, Raven, New York.

Steffens, G. J., Gunzler, W. A., Otting, F., Frankus, E., & Flohe, L. (1982) *Hoppe-Seyler's Z. Physiol. Chem. 363*, 1043–1058.

Steigemann, W. (1982) "PROTEIN", a Package of Crystallographic Programs for the Analysis of Proteins, Institut für Biochemie, Martiensried, BRD.

Thewes, T., Ramesh, V., Simplaceanu, E. L., & Llinás, M. (1988) *Eur. J. Biochem. 175*, 237–249.

Thorsen, S. (1975) *Biochim. Biophys. Acta 393*, 55–65.

Thorsen, S., Clemmensen, I., Sottrup-Jensen, L., & Magnusson, S. (1981) *Biochim. Biophys. Acta 668*, 377–387.

Trexler, M., Váli, Z., & Patthy, L. (1982) *J. Biol. Chem. 257*, 7401–7406.

Tulinsky, A., Park, C. H., & Skrypczak-Jankun, E. (1988a) *J. Mol. Biol. 202*, 885–901.

Tulinsky, A., Park, C. H., Mao, B., & Llinás, M. (1988b) *Proteins 3*, 85–96.

Urano, T., Chibber, B. A. K., & Castellino, F. J. (1987) *Proc. Natl. Acad. Sci. U.S.A. 84*, 4031–4034.

Urano, T., De Serrano, V. S., Gaffney, P. J., & Castellino, F. J. (1988) *Biochemistry 27*, 6522–6528.

Váli, Z., & Patthy, L. (1984) *J. Biol. Chem. 259*, 13690–13694.

Van Zonneveld, A. J., Veerman, H., & Pannekoek, H. (1986a) *J. Biol. Chem. 261*, 14214–14218.

Van Zonneveld, A. J., Veerman, H., & Pannekoek, H. (1986b) *Proc. Natl. Acad. Sci. U.S.A. 83*, 4670–4674.
Verheijen, J. H., Caspers, M. P. M., Chang, G. T. G., de Munk, G. A. W., Pouwels, P. W., & Enger-Valk, B. E. (1986) *EMBO J. 5*, 3525–3530.
Wang, B.-C. (1985) in *Methods in Enzymology* (Wyckoff, H. W., Hirs, C. H. W., & Timasheff, S. N., Eds.) Vol. 115, Part B, pp 90–112, Academic Press, Orlando, FL.
Weening-Verhoeff, E. J. D., Quax, P. H. A, Van Leeuwen, R. T. J., Rehberg, E. F., Marotti, K. R., & Verheijen, J. H. (1990) *Protein Eng. 4*, 191–198.
Wilmot, C. M., & Thornton J. M. (1988) *J. Mol. Biol. 203*, 221–232.
Winn, E. S., Hu, S.-P., Hochschwender, S. M., & Laursen, R. A. (1980) *Eur. J. Biochem. 104*, 579–586.
Wu, T.-P., Padmanabhan, K., Tulinsky, A., & Mulichak, A. M. (1991) *Biochemistry 30*, 10589–10594.
Wyckoff, H. W., Doscher, M., Tsernoglou, D., Inagami, T., Johnson, L. N., Hardman, K. D., Allewell, N. M., Kelly, D. M., & Richards, F. M. (1967) *J. Mol. Biol. 27*, 563–578.

Lipid Polymorphism: A Correction. The Structure of the Cubic Phase of Extinction Symbol *Fd--* Consists of Two Types of Disjointed Reverse Micelles Embedded in a Three-Dimensional Hydrocarbon Matrix†

Vittorio Luzzati,*,‡ Rodolfo Vargas,‡ Annette Gulik,‡ Paolo Mariani,§ John M. Seddon,∥ and Emilio Rivas⊥

Centre de Génétique Moléculaire, Laboratoire Propre du CNRS Associé à l'Université Pierre et Marie Curie, 91198 Gif-sur-Yvette, France, Istituto di Fisica Medica, Università di Ancona, Via Monte d'Ago, 60100 Ancona, Italy, Department of Chemistry, Imperial College, London SW7 2AY, U.K., and Instituto de Biología Celular, CONICET, Buenos Aires, Argentina

Received April 17, 1991; Revised Manuscript Received September 17, 1991

ABSTRACT: The X-ray scattering study of a cubic phase of extinction symbol *Fd--*, recently performed on a lipid extract (PFL) from *Pseudomonas fluorescens* [Mariani et al. (1990) *Biochemistry 29*, 6799–6810] has been extended to several other systems, all consisting of mixtures of water-miscible (MO, PC, PE, oleate) and of water-immiscible (FA, DG) lipids, plus water. In all of these systems the cubic phase was observed in the presence of excess water. Some inconsistencies observed between PFL and the other systems, the fact that in PFL one of the reflections of the cubic phase happened to coincide with the strongest reflection of the hexagonal phase, and the finding, in one of the original cubic samples of PFL kept in the cold for more than 3 years, that the intensity of one of the reflections had decreased dramatically all indicated that a nonnegligible amount of a hexagonal impurity was in fact present in the samples of PFL originally thought to contain a pure cubic phase. The intensities were corrected for that impurity and analyzed again using a pattern recognition approach based upon the axiom that the histogram of the electron density maps is invariant with respect to physical structure, when different phases are compared whose chemical composition is the same. The hexagonal phase provided the reference phase for the comparison. The moments $\langle(\Delta\rho)^n\rangle$ were used to compare the histograms. All the phase combinations (the φ-sets) compatible with the data were generated and were screened using the distance between the points of the cubic and the hexagonal phases in the 6D space of the moments ($[\langle(\Delta\rho)^n\rangle]^{1/n}$), with n = 3–8. The result of the analysis is a structure formed by two types of disjointed micelles of type II (water-in-oil), quasi-spherical in shape: eight (per F-centered cubic cell), of symmetry $\bar{4}3m$, are centered at positions a, and 16, of symmetry $\bar{3}m$, are centered at positions d [according to the *International Tables* (1952)]. This structure has previously been proposed by Charvolin and Sadoc (1988) on the basis of formal geometric arguments. The study of the cubic phase of the other lipid systems is hindered by the lack of a reference phase; the structure was analyzed by reference to the cubic phase of PFL and found to be the same in all the systems. This cubic phase is the first example, among lipid-containing phases, of a 3D periodically ordered micellar organization of type II.

A face-centered cubic phase of extinction symbol *Fd--* (cubic aspect 15; phase Q_{15}, according to our notation) was discovered by Tardieu (1972) in a lipid extract from *Pseudomonas fluorescens*, provided by E. Rivas. For a long time no other example of that phase was reported in any lipid-containing system. Quite recently, a renewed interest in cubic phases has stimulated a more systematic search that has uncovered several additional examples of that phase: MO–OA–water[1] (Mariani et al., 1988, 1990), DOPC–DOG–water (Seddon, 1990), NaO–OA–water (Seddon et al., 1990a), PE–DOG (Gulik and Vargas, unpublished work), some ill-

† This work was supported in part by grants from the Association Française pour la Recherche Médicale, the Ligue Nationale Française contre le Cancer, and the Science and Engineering Research Council (U.K.) (Research Grant GR/C/95428). One of us (R.V.) was supported by a postdoctoral grant from the Association Française pour la Recherche Médicale.

‡ Laboratoire Propre du CNRS Associé à l'Université Pierre et Marie Curie.
§ Università di Ancona.
∥ Imperial College.
⊥ CONICET.

[1] Abbreviations: PFL, lipid extract from *Pseudomonas fluorescens* (Mariani et al., 1990); MO, monoolein; FA, fatty acid; OA, oleic acid; MA, myristic acid; NaO, sodium oleate; PC, phosphatidylcholine (lecithin); PE, phosphatidylethanolamine; DOPC, dioleoylphosphatidylcholine; DMPC, dimyristoylphosphatidylcholine; DG, diacylglycerol; DOG, dioleoylglycerol. The lipids are arranged in two classes: water-miscible are those (PFL, MO, NaO, PC, PE, DOPC, DMPC) that display water-containing phases, and water-immiscible are the others (FA, OA, MA, DG, DOG).

0006-2960/92/0431-279$03.00/0